

Calendering of Non-Newtonian Fluids

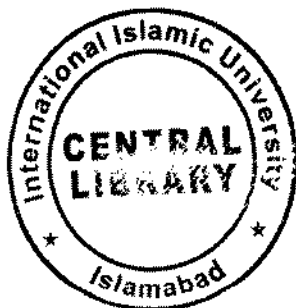


By

HAMMAD HUSSAIN

Department of Mathematics and Statistics
Faculty of Basic and Applied Sciences
International Islamic University, Islamabad
Pakistan

2015



Accession No IH-14826

K/C

MS

532

HAC

- Non newtonian fluid
- Fluid dynamics
- Albeses

Calendering of Non-Newtonian Fluids



By

HAMMAD HUSSAIN

Supervised by

Dr. NASIR ALI

Department of Mathematics and Statistics
Faculty of Basic and Applied Sciences
International Islamic University, Islamabad
Pakistan
2015

Calendering of Non-Newtonian Fluids

By

HAMMAD HUSSAIN

*A Thesis
Submitted in the Partial Fulfillment of the
Requirements for the Degree of
MASTER OF SCIENCE IN MATHEMATICS*

Supervised by

Dr. NASIR ALI

**Department of Mathematics and Statistics
Faculty of Basic and Applied Sciences
International Islamic University, Islamabad
Pakistan
2015**

Certificate

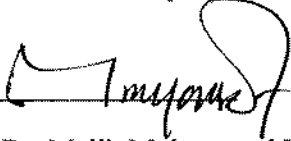
Calendering of Non-Newtonian Fluids

By

HAMMAD HUSSAIN

A THESIS SUBMITTED IN THE PARTIAL FULFILLMENT OF THE
REQUIREMENTS FOR THE DEGREE OF THE MASTRER OF SCIENCE IN
MATHEMATICS

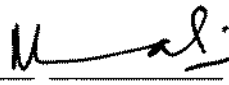
We accept this dissertation as conforming to the required standard.

1. 
Prof. Dr. Malik Muhammad Yousaf

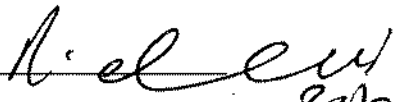
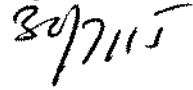
(External Examiner)

2. 
Dr. Ahmer Mehmood

(Internal Examiner)

3. 
Dr. Nasir Ali

(Supervisor)

4. 
Dr. Rahmat Ellahi 

(Chairman)

Department of Mathematics and Statistics

Faculty of Basic and Applied Sciences

International Islamic University, Islamabad

Pakistan

2015

Declaration

I hereby declare and affirm that this research work neither as a whole nor as a part has been copied out from any source. It is further declared that I have developed this research work entirely on the basis of my personal efforts.

Moreover, no portion of the work presented in this thesis has been submitted in support of an application for other degree of qualification in this or any other university or institute of learning.

Signature: _____



HAMMAD HUSSAIN

MS in Mathematics

Reg: No. 127-FBAS/MSMA/S-13

DEDICATED

To

My Honorable Mother and Loving Father.

Caring Brother & Sisters

Respected Teachers

And

My Friends

**"If you wish for a pearl
You must leave the desert
And even if you never find
The gleaming pearl, at least**

You won't have failed to reach the water".

[From Hakim Sanai: Hadiqat al-Haqiqa (walled garden of truth)].

Acknowledgement

I am greatly thankful to **Almighty ALLAH** who is the most beneficent and the most merciful provided me the enough strength to achieve my goal to a thesis. I offer Darood Pak to my beloved **prophet Muhammad (SAW)** whose teachings bring the strength and ability to learn more and more.

I would like to put a record on my appreciations and gratitude to all who have rendered their support and input. Without them it would not be possible for me to shape this study particularly, I would like to show my gratitude to my beloveds, kind natured, competent, dedicated, prominent and devoted supervisor **Dr. Nasir Ali** for sharing his pearls of wisdom with me during the source of research.

I also acknowledge with a deep sense of reverence my gratitude towards my parents, my elder brother and my sisters who have always support me morally as well as economically. At last but not least gratitude to all my friends specially. **Rana Asif** who directly or indirectly helped me to complete this thesis work. Last, but not the least, my family who continuously supported and encouraged me during my work and the power of the sincere prayers and good wishes of my parents especially my greatest Mother, I particularly thank my brother for love and care during my work. I also thank my friends and all nears dears who led me to the path of success in my research work. I thank all of you.

HAMMAD HUSSAIN

Preface

Calendering is a process in which a polymer material is pushed ahead through the narrow region between two rotating rolls in such a way as to produce a thin sheet. This mechanism is extensively studied in the past few decades. The pioneering theoretical studies on calendering were carried out by Gaskell [1] and Mekelvey [2] for the Newtonian case. The text book of Middleman [3] also reports the results of calendering for Newtonian and power-law fluids. Sofou and Mitsoulis [4] employed lubrication theory to study the calendering of viscoplastic sheets. Numerical investigation of shape of free surfaces of entering and exiting sheets to calender viscoelastic sheets with a finite thickness was carried out by Mitsoulis [5]. The combined effects of asymmetry and viscous heating for the non isothermal nip flow in calendering were considered by Dobbels and Mewis [6]. In addition, the effect of viscous dissipation on the calendering process of Newtonian and power-law fluids has been studied by Kiparissides and Vlachopoulos [7]. Recently, the influence of the temperature-dependent consistency index on the exiting sheet thickness in the calendering process of a power law fluid was reported by Arcos et al. [8], and they found a decrease of about 6.91% for the calendered thickness. In all the works reported above, the fluids are not viscoelastic in the usual sense, because they have no memory. Accordingly, Zheng and Tanner [9] carried out an analysis of the calendering process using the power-law and the Simplified Phan-Thien-Tanner fluid models. The authors focused on determining the separation criterion at the roll exit plane. For the viscoelastic case, they determined the separation point using the criterion of zero tangential traction. As a fundamental result, they determined that unlike the inelastic case, the sheet was found to be thicker after leaving the nip. More recently Arcos et al. [10] presented a theoretical analysis of the calendering exiting thickness of viscoelastic sheets using Simplified Phan-Thien-Tanner model. They are followed by Siddique et al. [11] who provided the analysis of

flow in a calendering process using the constitutive equation of third order fluid. The dissertation is based the review of the two papers by Siddique et al. [11] and Arcos et al. [10].

Chapter 1 is introduction in nature and includes some basic definition and equations. The result of Siddique et al. [11] are reproduced in detail in chapter 2. Chapter 3 is a detailed review of work carried out Arcos et al. [10].

Contents

1 Preliminaries	4
1.1 Basic definitions and concepts in fluid mechanics	4
1.1.1 Fluid	4
1.1.2 Flow	4
1.1.3 Distortion	4
1.1.4 Fluid mechanics	5
1.1.5 Viscosity	5
1.1.6 Gradient of velocity	5
1.1.7 Divergence of a vector	5
1.1.8 Divergence of a tensor	6
1.1.9 Pressure	6
1.1.10 Newton's law of viscosity	6
1.2 Classification of fluids	6
1.2.1 Inviscid fluids	6
1.2.2 Real fluids	7
1.3 Types of flow	7
1.3.1 Laminar flow	7
1.3.2 Turbulent flow	8
1.3.3 Uniform flow	8
1.3.4 Non-uniform flow	9
1.3.5 Steady flow	9

1.3.6	Unsteady flow	9
1.3.7	Compressible flow	9
1.3.8	Incompressible flow	9
1.3.9	Rotational and irrotational flow	9
1.4	Dimensionless numbers	10
1.4.1	Weissenberg number	10
1.4.2	Reynolds number	10
1.5	Fundamental equations	10
1.5.1	Continuity equation	10
1.5.2	Equation of motion	10
1.6	Navier-Stokes equation	11
1.7	Techniques of solution	11
1.7.1	Perturbation method	11
1.7.2	Runge-Kutta method	12
1.8	Calendering	13
2	Analysis of flow of third-order fluid in calendering process	14
2.1	Governing equations	14
2.1.1	Dimensionless formulation	18
2.1.2	Flow rate and sheet thickness	19
2.2	Perturbation solution	20
2.2.1	System of zeroth-order	20
2.2.2	System of first-order	20
2.2.3	Solution of zeroth-order system	21
2.2.4	Solution for first-order system	22
2.3	Results and discussion	24

3	Theoretical analysis of calendering of Phan-Thien-Tanner fluid	29
3.1	Formulation	29
3.2	Dimensionless equations	31
3.3	Perturbation solution	33
3.3.1	System of zeroth-order	33
3.3.2	System of first-order	33
3.3.3	Zeroth-order solution	34
3.3.4	First-order solution	35
3.4	Numerical solution	37
3.5	Roll separating force	39
3.6	Power input	39
3.7	Graphical results and discussion	40

Chapter 1

Preliminaries

This chapter includes some basic definition and fundamental equations.

1.1 Basic definitions and concepts in fluid mechanics

1.1.1 Fluid

A substance (material) that distorted is continuously under the influence of some external stress is called fluid.

1.1.2 Flow

A substance (material) goes under distortion when some external forces applied on it. If distortion increases continuously, the phenomena is called flow.

1.1.3 Distortion

It is relative change in position or length of the fluid particle.

1.1.4 Fluid mechanics

Fluid Mechanics is that branch of mechanics in which we deal with the behavior of fluids either at rest or in motion.

1.1.5 Viscosity

A measure of resistance to flow when the fluid is in motion is called viscosity of that fluid. It is usually denoted by μ .

1.1.6 Gradient of velocity

Let $\mathbf{V}(x_i, t)$, $i = 1, 2, 3$ where x_i are the Cartesian coordinates, denotes the velocity field for the fluid in motion. Then we define the gradient of velocity field as

$$\nabla \mathbf{V} = e_i e_j \frac{\partial v_j}{\partial x_i}, \quad (1.1)$$

which in matrix form becomes

$$\nabla \mathbf{V} = \begin{bmatrix} \frac{\partial v_1}{\partial x_1} & \frac{\partial v_1}{\partial x_2} & \frac{\partial v_1}{\partial x_3} \\ \frac{\partial v_2}{\partial x_1} & \frac{\partial v_2}{\partial x_2} & \frac{\partial v_2}{\partial x_3} \\ \frac{\partial v_3}{\partial x_1} & \frac{\partial v_3}{\partial x_2} & \frac{\partial v_3}{\partial x_3} \end{bmatrix}. \quad (1.2)$$

where $v_i, i = 1, 2, 3$ are the components of velocity field \mathbf{V} .

1.1.7 Divergence of a vector

Its expressed as

$$\nabla \cdot \mathbf{V} = \sum \frac{\partial v_i}{\partial x_i} = \frac{\partial v_1}{\partial x_1} + \frac{\partial v_2}{\partial x_2} + \frac{\partial v_3}{\partial x_3}. \quad (1.3)$$

1.1.8 Divergence of a tensor

For an arbitrary tensor \mathbf{S} of order two, it is defined as

$$\nabla \cdot \mathbf{S} = e_j \frac{\partial S_{ij}}{\partial x_i}, \quad (1.4)$$

where S_{ij} are the components of \mathbf{S} .

1.1.9 Pressure

Pressure p is the magnitude of the normal force F per unit surface area A . It is a scalar quantity. Mathematically

$$p = \frac{F}{A}. \quad (1.5)$$

1.1.10 Newton's law of viscosity

Let us consider motion of fluid between two parallel surface generated by the motion of upper surface. Let $u_1(x_2)$ be the component of fluid velocity in x_1 - direction. Then Newton's law of viscosity states that the shear stress is directly and linearly proportional to the rate of deformation. Mathematically, we can write

$$\tau = \mu \frac{du_1}{dx_2} \quad (1.6)$$

where τ is the shear stress and du_1/dx_2 is the deformation rate.

1.2 Classification of fluids

Generally, fluids can be classified into following types.

1.2.1 Inviscid fluids

Fluids of zero or negligible viscosity falls in the category of inviscid fluids. Such can exert only normal stress (pressure) on a submerged surface.

1.2.2 Real fluids

Real fluids are those fluids for which viscosity is finite. A real fluid can exert tangential (shearing) stress in addition to normal stress on a submerged surface.

Real fluids are further divided into two categories.

Newtonian fluid

All real fluids that obey the Newton's law of viscosity are known as Newtonian fluids.

Non-Newtonian fluid

All such fluids in which shear stress is non-linearly proportional to velocity gradient are known as non-Newtonian fluids. For unidirectional motion of such fluids, we can write

$$\tau = k \left(\frac{\partial u_1}{\partial x_2} \right)^n, \quad (1.7)$$

where k is the consistency index and n is called power-law index. For $n = 1$, the above relation reduce to Newton's law of viscosity.

1.3 Types of flow

Flows are broadly classified in following types,

1.3.1 Laminar flow

A flow in which fluid particles move in straight lines is said to be laminar. In this flow path of individual particles do not intersect with each other.

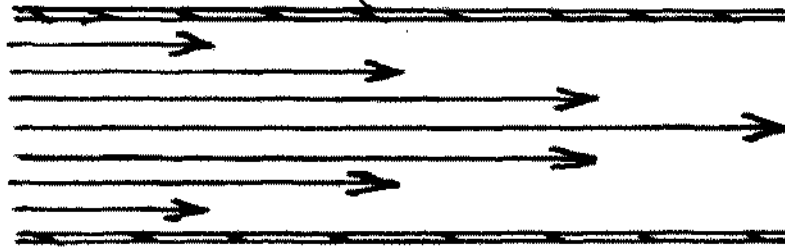


Fig 1.1: Laminar flow representation

1.3.2 Turbulent flow

A flow in which fluid particles moves in irregular fashion in all direction is said to be turbulent. In this flow path of individual fluid particle intersect with each other.

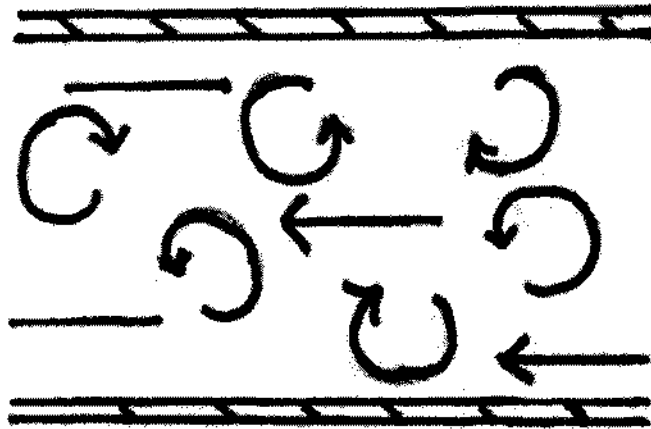


Fig 1.2: Turbulent flow representation

1.3.3 Uniform flow

A flow in which flow characteristics do not change from point to point is said to be uniform.

1.3.4 Non-uniform flow

A flow in which flow properties changes from point to point is said to be non-uniform.

1.3.5 Steady flow

A flow is said to be steady in which fluid properties do not change with respect to time. For such a flow

$$\frac{\partial \eta}{\partial t} = 0. \quad (1.8)$$

where η represents any fluid property.

1.3.6 Unsteady flow

The flow is regarded as unsteady if the fluid properties changes with respect to time i.e.

$$\frac{\partial \eta}{\partial t} \neq 0. \quad (1.9)$$

1.3.7 Compressible flow

A flow in which there are no changes in density is known as compressible flow. Flows of gases are compressible in nature.

1.3.8 Incompressible flow

A flow is said to be incompressible in which density remains constant. Flows of liquids are generally incompressible.

1.3.9 Rotational and irrotational flow

If individual fluid particles rotate about their own axes during the flow, then flow is known a rotational. Otherwise, it is irrotational. Mathematically, for irrotational flow

$$\nabla \times \vec{V} = 0. \quad (1.10)$$

1.4 Dimensionless numbers

1.4.1 Weissenberg number

The Weissenberg number We is a dimensionless number used in the study of viscoelastic flows and named after Karl Weissenberg. It is the ratio of the relaxation time of the fluid and a specific process time.

1.4.2 Reynolds number

It is the ratio of inertia force to the viscous force. It is denoted by Re .

1.5 Fundamental equations

The motion of fluid whether Newtonian or non-Newtonian can be analyzed using the following equations.

1. Continuity equation
2. Equation of motion

1.5.1 Continuity equation

The equation of continuity is based on the law of conservation of mass which states that the mass of a closed system remains constant. Mathematically it is expressed as

$$\frac{\partial \rho}{\partial t} + \nabla \cdot (\rho \mathbf{V}) = 0, \quad (1.11)$$

where ρ is fluid density.

1.5.2 Equation of motion

The equation of motion is based on law of conservation of momentum. In mathematical form it is expressed as

$$\rho \frac{d\mathbf{V}}{dt} = \text{div}\mathbf{T} + \rho b, \quad (1.12)$$

where \mathbf{T} is stress tensor, b is body force and

$$\frac{d}{dt} = \frac{\partial}{\partial t} + \mathbf{V} \cdot \nabla. \quad (1.13)$$

is the material derivative.

1.6 Navier-Stokes equation

The equation of motion for Newtonian fluids is generally known as Navier-Stokes equation. For Newtonian fluids

$$\mathbf{T} = -P\delta_{ij} + \mu \left(\nabla\mathbf{V} + \nabla\mathbf{V}^\dagger \right), \quad (1.14)$$

where † denotes transpose and δ_{ij} is the identity tensor. Inserting (1.14) in (1.12), we get

$$\rho \frac{Du_i}{Dt} = \rho f_i - \frac{\partial P}{\partial x_i} + \frac{\partial}{\partial x_j} \left[\mu \left(\frac{\partial u_i}{\partial x_j} + \frac{\partial u_j}{\partial x_i} - \frac{2}{3} \delta_{ij} \frac{\partial u_k}{\partial x_k} \right) \right]. \quad (1.15)$$

1.7 Techniques of solution

There are numerous of techniques to solve differential equations. Two of them namely; perturbation method and Runge-kutta method are described below.

1.7.1 Perturbation method

The most powerful technique to solve nonlinear partial differential equations is perturbation method. Perturbation method leads to an expression for desired solution in term of power series in some small parameter called perturbation series. The leading term in this power series is the solution of exact solvable problem. In this technique we assume a very small physical parameter, expand the dependent variables in power series of small parameter and then put this series into original equation(s) and conditions (boundary and initial). After equating the

terms corresponding to power of small parameter, one get system of linear differential equation. Solving such system sequentially one gets the solution of the original problem.

1.7.2 Runge-Kutta method

Runge-Kutta method are single step method with multiple stages per step. It is a most popular ODE solver. It is an iterative methods and important family of implicit and explicit method which are used for numerical solutions of an differential equations, this methods were developed by German mathematician C.Runge and M.Kutta in 1900. Modern development in this method are mostly in 1960s. In this method, we will use iterative scheme which depends upon different values of k , where k are the known stages of R-K method. To solve any differential equation we have to know the value of x_0 . Scheme of second order Runge-Kutta method is described below

$$f(x_n + 1) = f(x_n) + \frac{1}{6}(k_1 + 2k_2 + 2k_3 + k_4), \quad (1.22)$$

where

$$k_1 = hf(x_n), \quad (1.23)$$

$$k_2 = hf\left(x_n + \frac{h}{2}\right), \quad (1.24)$$

$$k_3 = hf\left(x_n + \frac{h}{2}\right), \quad (1.25)$$

$$k_4 = hf(x_n + h), \quad (1.26)$$

clearly

$$k_2 = k_3 = k, \quad (1.27)$$

then generalized form will be

$$f(x_n + 1) = f(x_n) + \frac{1}{6}(k_1 + 4k + k_4). \quad (1.28)$$

It requires four evaluation of the function f per time step.

1.8 Calendering

The term “Calender” is derived from the Greek word *Kylindros* which means cylinder and according to the Webster’s International Dictionary it means to press as cloth, rubber, paper between roller in order to make smooth and glossy (shinning). It is the process of forming a flowable material into sheet by passing it between two or more rotating cylinders. Fluid flow between rotating cylinders is the physical basis of calendering process We shall describe in detail such flow for two different materials in chapter two and three, respectively.

Chapter 2

Analysis of flow of third-order fluid in calendering process

In this chapter, we review the work of Siddique et al. [11] where the authors have analyzed the flow of non-Newtonian material when it is dragged through a narrow region between two co-rotating rolls. The mass and momentum conservation equations are non-dimensionalized and solved for the velocity and pressure using the perturbation method. The dimensionless leave-off distance in calendering process is expressed in term of eigen value problem. Various operating variables such as maximum pressure, the roll separating force, power transmitted to the fluid by the rolls are also calculated.

2.1 Governing equations

The law of mass and momentum for an incompressible flow of a third-order are

$$\nabla \cdot \mathbf{V} = 0, \quad (2.1)$$

$$\rho \frac{d\mathbf{V}}{dt} = -\nabla p + \text{div} \mathbf{S}, \quad (2.2)$$

where \mathbf{S} is the extra stress tensor. For third-order fluid

$$\mathbf{S} = \mu \mathbf{A}_1 + \alpha_1 \mathbf{A}_2 + \alpha_2 \mathbf{A}_1^2 + \beta_1 \mathbf{A}_3 + \beta_2 (\mathbf{A}_1 \mathbf{A}_2 + \mathbf{A}_2 \mathbf{A}_1) + \beta_3 (\text{tr} \mathbf{A}_1^2) \mathbf{A}_1, \quad (2.3)$$

where $\alpha_i (i = 1, 2)$ and $\beta_i (i = 1, 2, 3)$ are the material constant of third-order fluid and $\mathbf{A}_i = (1, 2, 3)$ is the i th Rivlin-Erickon tensor. The first Rivlin-Erickon tensor is defined as

$$\mathbf{A}_1 = (\nabla \mathbf{V}) + (\nabla \mathbf{V})^\dagger, \quad (2.4)$$

while higher order tensor are given by the following formula

$$\mathbf{A}_n = \left(\frac{\partial}{\partial t} + (\mathbf{V} \cdot \nabla) \right) \mathbf{A}_{n-1} + \mathbf{A}_{n-1} (\nabla \mathbf{V}) + (\nabla \mathbf{V})^\dagger \mathbf{A}_{n-1} \cdot n > 1. \quad (2.5)$$

It has been proved by Fosdick and Rajagopal.[12] that for a thermodynamically compatible third-order fluid the material parameter must fulfill the following constraints:

$$\beta_1 = \beta_2 = 0, \quad -\sqrt{24\mu\beta_3} \leq \alpha_1 + \alpha_2 \leq \sqrt{24\mu\beta_3}, \quad \mu \geq 0, \quad \alpha_1 \geq 0, \quad \beta_3 \geq 0. \quad (2.6)$$

In view of above constraints model (2.3) reduce to

$$\mathbf{S} = \mu \mathbf{A}_1 + \alpha_1 \mathbf{A}_2 + \alpha_2 \mathbf{A}_1^2 + \beta_1 \mathbf{A}_3 + \beta_3 (\text{tr} \mathbf{A}_1^2) \mathbf{A}_1, \quad (2.7)$$

Substituting Eq. (2.7) in Eq. (2.2) and using the definition (2.4) and (2.5), we may find

$$\begin{aligned} -\nabla p + \mu \nabla^2 \mathbf{V} + \alpha_1 \left[\nabla^2 \mathbf{V}_t + \nabla^2 (\nabla \times \mathbf{V}) \times \mathbf{V} + \nabla \left(\mathbf{V} \cdot \nabla^2 \mathbf{V} + \frac{1}{4} |\mathbf{A}_1|^2 \right) \right] \\ + (\alpha_1 + \alpha_2) \nabla \cdot \mathbf{A}_1^2 + \beta_3 \mathbf{A}_1 \nabla |\mathbf{A}_1|^2 + \beta_3 |\mathbf{A}_1|^2 \nabla^2 \mathbf{V} = \rho \frac{D\mathbf{V}}{Dt}. \end{aligned} \quad (2.8)$$

For two dimensional flows like calendaring, we define

$$\mathbf{V} = [u_1(x_1, x_2), u_2(x_1, x_2), 0]. \quad (2.9)$$

For the subsequent analysis, we replace u_1, u_2 by u, v and x_1, x_2 by x, y .

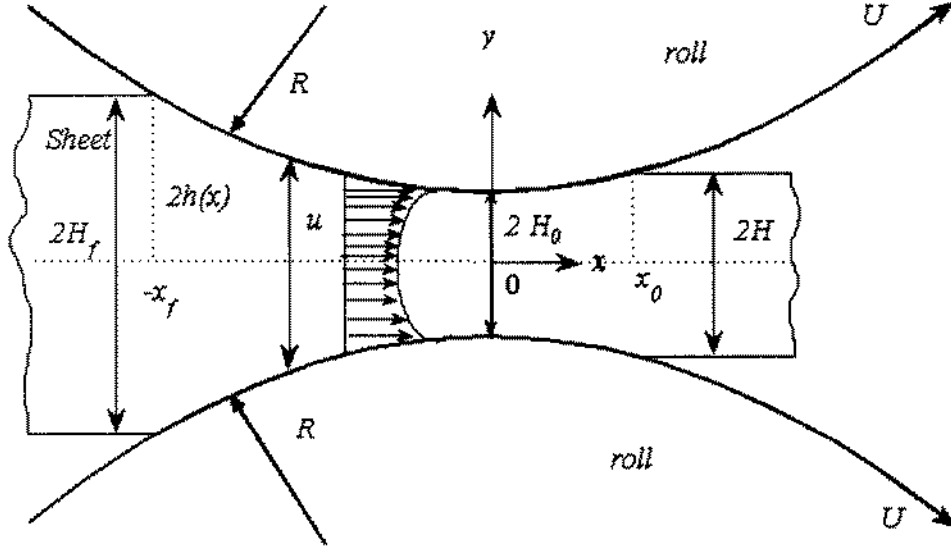


Fig.1. Schematic diagram of flow problem.

using the above definition of velocity in Eq. (2.8), we get

$$\frac{\partial u}{\partial x} + \frac{\partial v}{\partial y} = 0, \quad (2.10)$$

$$\frac{\partial h}{\partial x} + v(-\rho\psi + \alpha_1 \nabla^2 \psi) + \mu \frac{\partial \psi}{\partial y} + \beta_3 \frac{\partial}{\partial y} (\psi M) - 2\beta_3 \left\{ \left(\frac{\partial u}{\partial x} \frac{\partial}{\partial x} + \frac{\partial v}{\partial x} \frac{\partial}{\partial y} \right) \right\} = 0, \quad (2.11)$$

$$\frac{\partial h}{\partial y} - v(-\rho\psi + \alpha_1 \nabla^2 \psi) - \mu \frac{\partial \psi}{\partial y} - \beta_3 \frac{\partial}{\partial x} (\psi M) - 2\beta_3 \left\{ \left(\frac{\partial u}{\partial y} \frac{\partial}{\partial x} + \frac{\partial v}{\partial y} \frac{\partial}{\partial y} \right) \right\} = 0, \quad (2.12)$$

where

$$\psi = \frac{\partial v}{\partial x} + \frac{\partial u}{\partial y}, \quad (2.13)$$

$$h = \frac{\rho}{2} q^2 - \alpha_1 (u \nabla^2 u + v \nabla^2 v) - \left(\frac{3\alpha_1 + 2\alpha_2}{4} \right) M + p, \quad (2.14)$$

$$M = Tr \left(\mathbf{A}_1 \mathbf{A}_2^\dagger \right), \quad (2.15)$$

and

$$q^2 = u^2 + v^2. \quad (2.16)$$

In the nip region the following approximations are valid

$$v \ll u \text{ and } \frac{\partial}{\partial x} \ll \frac{\partial}{\partial y}. \quad (2.17)$$

In order to find the characteristics scales for velocity and pressure, we define the following scales for x, y and u .

$$x \sim L_c, y \sim H_0, u \sim U. \quad (2.18)$$

The equation of continuity (2.1) along with (2.18) allows us to write

$$\frac{v_c}{U} \sim \frac{H_0}{L_c} \ll 1. \quad (2.19)$$

From (2.19), it is found that magnitude of transversal velocity, v_c is smaller than the longitudinal velocity. A balancing between pressure and other terms yields

$$P_c \sim \sqrt{\frac{2R}{H_0}} \frac{\mu_0}{\rho f^c p H_0}. \quad (2.20)$$

In view of the above discussion, Eqs. (2.10) – (2.12) are reduces to:

$$\frac{\partial u}{\partial x} = 0, \quad (2.21)$$

$$\frac{\partial^2 u}{\partial y^2} + \frac{2\beta_3}{\mu} \frac{\partial}{\partial y} \left(\frac{\partial u}{\partial y} \right)^3 = \frac{1}{\mu} \frac{\partial P}{\partial x}, \quad (2.22)$$

$$\frac{\partial P}{\partial y} = 0, \quad (2.23)$$

where

$$P = p - (\alpha_1 + \alpha_2) \left(\frac{\partial u}{\partial y} \right)^2 \quad (2.24)$$

is the modified pressure. The appropriate boundary condition to be satisfied by the velocity component u are:

$$\begin{cases} u = & \text{on } y = h(x), \\ \frac{\partial u}{\partial y} = 0 & \text{on } y = 0, \end{cases} \quad (2.25)$$

where l is the linear velocity of the roll. The height of the roll surface from the center line is defined as

$$h(x) = H_0 + R - (R^2 - x^2)^{1/2}. \quad (2.26)$$

Since, it is intended to perform the analysis for $x \ll R$, therefore $h(x)$ may be approximated as

$$h(x) = H_0 \left(1 + \frac{x^2}{2H_0R} \right). \quad (2.27)$$

2.1.1 Dimensionless formulation

Let us introduce the following dimensionless variables

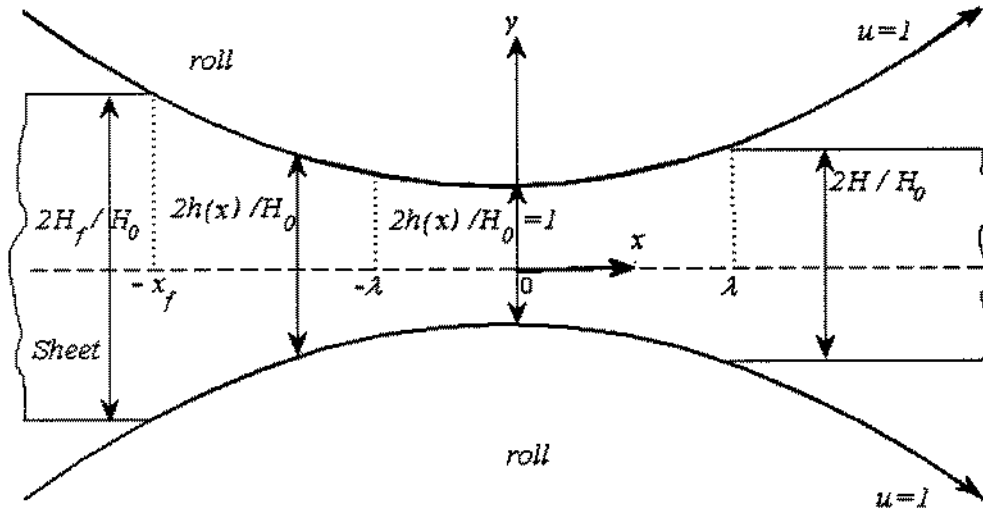


Fig. 2. Representation of flow geometry in dimensionless variables.

$$x^* = \frac{x}{\sqrt{2RH_0}}, u^* = \frac{u}{H_0}, y^* = \frac{y}{H_0}, P^* = \sqrt{\frac{H_0}{2R}} \frac{pH_0}{\mu U} = \frac{2\beta_3}{\mu H_0}, h^*(x^*) = \frac{h(x)}{H_0}. \quad (2.28)$$

Using (2.28) the governing Eq. (2.22) and boundary conditions (2.25) take the form

$$\frac{\partial^2 u}{\partial y^2} + \beta \frac{\partial}{\partial y} \left(\frac{\partial u}{\partial y} \right)^3 = \frac{dp}{dx}. \quad (2.29)$$

$$\begin{cases} u = 1 & \text{on } y = h(x) = 1 + x^2 \\ \frac{\partial u}{\partial y} = 0 & \text{on } y = 0 \end{cases} \quad (2.30)$$

where * are omitted for brevity. The standard condition to be satisfied by the pressure and pressure gradient are

$$\begin{cases} \frac{dP}{dx} = P = 0 & \text{at } x = \lambda \\ P = 0 & \text{at } x = -x_f \end{cases} \quad (2.31)$$

where λ is the dimensionless leave-off and $-x_f$ is the entry point where sheet first bites the rolls.

2.1.2 Flow rate and sheet thickness

The volumetric flow rate in dimensional form reads

$$Q = 1 + \lambda^2 = \int_0^{1+x^2} u dy \quad (2.32)$$

where λ is an eigen value of the problem. The following are the two flow regions based on the sign of pressure gradient.

- $-x_f \leq x \leq -\lambda$ where $dp/dx > 0$
- $-\lambda \leq x \leq \lambda$ where $dp/dx < 0$

The relation between x_f and entering sheet thickness is

$$x_f = \left(\frac{H_f}{H_0} - 1 \right)^{1/2}. \quad (2.33)$$

The expression relating exiting sheet thickness with λ is

$$\frac{H}{H_0} = 1 + \lambda^2. \quad (2.34)$$

2.2 Perturbation solution

In view of the nonlinear nature of the governing equation (2.29), the perturbation method will be employed for the analytical solution. To this end, the quantities u , P , Q , and λ are expressed as

$$u(x, y) = u_0(x, y) + \beta u_1(x, y) + \dots, \quad (2.35)$$

$$P(x) = P_0(x) + \beta P_1(x) + \dots, \quad (2.36)$$

$$Q = Q_0 + \beta Q_1 + \dots, \quad (2.37)$$

$$\lambda = \lambda_0 + \beta \lambda_1 + \dots \quad (2.38)$$

Substitution of above expressions in Eqs. (2.30) – (2.33) yields the following system at various orders of β :

2.2.1 System of zeroth-order

$$\frac{dP_0}{dx} = \frac{\partial^2 u_0}{\partial y^2}, \quad (2.39)$$

$$Q_0 = 1 + \lambda_0^2 = \int_0^{1+x^2} u_0 dy \quad (2.40)$$

$$\left\{ \begin{array}{l} \frac{\partial u_0}{\partial y} = 0 \quad \text{at } y = 0, \\ u_0 = 1 \quad \text{at } y = 1 + x^2, \\ \frac{dP_0}{dx} = P_0 = 0 \quad \text{at } x = \lambda_0. \end{array} \right. \quad (2.41)$$

2.2.2 System of first-order

$$\frac{dP_1}{dx} = \frac{\partial^2 u_1}{\partial y^2} + \frac{\partial}{\partial y} \left(\frac{\partial u_0}{\partial y} \right)^3, \quad (2.42)$$

$$Q_1 = 1 + 2\lambda_0\lambda_1 = \int_0^{1+x^2} u_1 dy, \quad (2.43)$$

$$\begin{cases} \frac{\partial u_1}{\partial y} = 0 & \text{at } y = 0, \\ u_1 = 1 & \text{at } y = 1 + x^2, \\ \frac{dP_1}{dx} = P_1 = 0 & \text{at } x = \lambda_1. \end{cases} \quad (2.44)$$

2.2.3 Solution of zeroth-order system

Solving Eq. (2.39) subject to boundary conditions (2.41), we get

$$u_0 = 1 + \frac{1}{2} \frac{dP_0}{dx} \left[y^2 - \left((1+x^2)^2 \right) \right]. \quad (2.45)$$

Utilizing (2.45) in (2.40) and performing the integration,

$$1 + \lambda_0 = \int_0^{1+x^2} u_0 dy$$

The expression for zeroth-order pressure gradient turn out to be

$$\frac{dP_0}{dx} = \frac{-3(\lambda_0^2 - x^2)}{(1+x^2)^3}, \quad -x_f \leq x \leq \lambda_0. \quad (2.46)$$

Integration of above expression gives

$$P_0(x) = \frac{3}{8} \left[\frac{x^2(1-3\lambda_0^2) - 1 - 5\lambda_0^2 x}{(1+x^2)^2} + (1-3\lambda_0^2) \left(\arctan(x) - \arctan\left(\sqrt{\frac{H_f}{H_0} - 1}\right) \right) + \frac{\left(\frac{H_f}{H_0}\right)(1-3\lambda_0^2) - 2(1+\lambda_0^2)}{\left(\frac{H_f}{H_0}\right)^2} \sqrt{\frac{H_f}{H_0} - 1} \right]. \quad (2.47)$$

In view of (2.46) the expression of zeroth-order velocity u_0 becomes

$$u_0(xy) = 1 + \frac{3(x^2 - \lambda_0^2)}{2(1+x^2)^3} \left[y^2 - (1+x^2)^2 \right]. \quad (2.48)$$

The unknown eigen value of the problem λ_0 can be found by evaluating the expression (2.48) in the limiting case $P_0 \rightarrow 0$ as $x \rightarrow -\infty$ and keeping the fact in mind that H_f/H_0 is known.

This gives $\lambda_0 = 0.4751$.

2.2.4 Solution for first-order system

Substitution of (2.48) in (2.42) yield the following determining equation for u_1 :

$$\frac{\partial^2 u_1}{\partial y^2} = \frac{dP_1}{dx} - \frac{81 (x^2 - \lambda_0^2)^3 y^2}{(1+x^2)^9}. \quad (2.49)$$

Twice integrating and using the boundary conditions (2.44), we find

$$u_1 = \frac{dP_1}{dx} \frac{1}{2} (y^2 - (1+x^2)^2) + \frac{27 (x^2 - \lambda_0^2)^3}{4 (1+x^2)^5} ((1+x^2)^4 - y^4). \quad (2.50)$$

From (2.43) and (2.50), we get

$$\frac{dP_1}{dx} = \frac{81}{5} \left[\frac{(x^2 - \lambda_0^2)^3}{(1+x^2)^7} - \frac{(\lambda_1^2 - \lambda_0^2)^3}{(1+x^2)^3 (1+\lambda_1^2)^4} \right], \quad -x_f \leq x \leq \lambda_1. \quad (2.51)$$

Now to obtain the expression of P_1 , we integrate the expression

$$P_1(x) = \frac{81}{5} \int_{-x_f}^x \left[\frac{(x^2 - \lambda_0^2)^3}{(1+x^2)^7} - \frac{(\lambda_1^2 - \lambda_0^2)^3}{(1+x^2)^3 (1+\lambda_1^2)^4} \right] dx, \quad (2.52)$$

and get

$$\begin{aligned} P_1(x) = & 0.0129 \arctan(x) - (6.0750\lambda_1^6 - 4.1137\lambda_1^4 + 0.9285\lambda_1^2 - 0.0699) \left(\frac{\arctan(x)}{(1+\lambda_1^2)^4} \right) + \\ & + \left(\frac{-2.4860}{(1+x^2)^6} + \frac{4.5669}{(1+x^2)^5} - \frac{2.3084}{(1+x^2)^4} + \frac{0.0069}{(1+x^2)^3} + \frac{0.0086}{(1+x^2)^2} + \frac{0.0129}{(1+x^2)} \right) x + \\ & + \left(\left(\frac{4.0500}{(1+x^2)^2} + \frac{6.0750}{(1+x^2)^2} \right) \lambda_1^6 - \left(\frac{2.7424}{(1+x^2)^2} + \frac{4.1137}{(1+x^2)^2} \right) \lambda_1^4 + \left(\frac{0.6190}{(1+x^2)^2} + \frac{0.9285}{(1+x^2)^2} \right) \lambda_1^2 \right) \end{aligned}$$

$$\begin{aligned}
& - \left(\frac{0.0466}{(1+x^2)^2} + \frac{0.0699}{(1+x^2)^2} \right) \frac{x}{(1+\lambda_1)^4} - 0.0129 \arctan \left(\sqrt{\frac{H_f}{H_0}} - 1 \right) + 6.0750\lambda_1^6 - 4.1137\lambda_1^4 \\
& + 0.9285\lambda_1^2 - 0.0699 \frac{\arctan \left(\sqrt{\frac{H_f}{H_0}} - 1 \right)}{(1+\lambda_1^2)^4} - \left(\frac{-2.4860}{\left(\frac{H_f}{H_0}\right)^6} + \frac{4.5669}{\left(\frac{H_f}{H_0}\right)^5} - \frac{2.3084}{\left(\frac{H_f}{H_0}\right)^4} \right. \\
& \left. + \frac{0.0069}{\left(\frac{H_f}{H_0}\right)^3} + \frac{0.0086}{\left(\frac{H_f}{H_0}\right)^2} + \frac{0.0129}{\left(\frac{H_f}{H_0}\right)} \right) \left(\sqrt{\frac{H_f}{H_0}} - 1 \right) + \left(\left(\frac{4.0500}{\left(\frac{H_f}{H_0}\right)^2} + \frac{6.0750}{\left(\frac{H_f}{H_0}\right)} \right) \lambda_1^6 \right. \\
& \left. - \left(\frac{2.7424}{\left(\frac{H_f}{H_0}\right)^2} + \frac{4.1137}{\left(\frac{H_f}{H_0}\right)} \right) \lambda_1^4 + \left(\frac{0.6190}{\left(\frac{H_f}{H_0}\right)^2} + \frac{0.9285}{\left(\frac{H_f}{H_0}\right)} \right) \lambda_1^2 - \left(\frac{0.0466}{\left(\frac{H_f}{H_0}\right)^2} + \frac{0.0699}{\left(\frac{H_f}{H_0}\right)} \right) \right) \frac{\left(\sqrt{\frac{H_f}{H_0}} - 1 \right)}{(1+\lambda_1^2)^4}.
\end{aligned} \tag{2.53}$$

The final expression of velocity can be obtained substituting the expression of dP_1/dx in (2.50) i.e.

$$u_1(xy) = \frac{81}{10} \left[\frac{(x^2 - \lambda_0^2)^3}{(1+x^2)^7} - \frac{(\lambda_1^2 - \lambda_0^2)^3}{(1+x^2)^3 (1+\lambda_1^2)^4} \right] \left(y^2 - (1+x^2)^2 \right) + \frac{27}{4} \frac{(x^2 - \lambda_0^2)^3}{(1+x^2)^5} \left((1+x^2)^4 - y^4 \right). \tag{2.54}$$

Assuming that H_f/H_0 is known and taking the limit of the expression (2.53) $P_1 \rightarrow 0$ as $x \rightarrow -\infty$, we get $\lambda_1 = 0.3336$.

The formulas for engineering quantities of interest which include roll separating force and power input are given below:

Roll separating force

$$\zeta = \int_{-\infty}^{\lambda} P(x) dx.$$

Power input

$$\wp = \int_{-\infty}^{\lambda} S_{xy}(x, 1) dx.$$

2.3 Results and discussion

The velocity profile u for different values of non-Newtonian parameter at eight different locations $x = -0.5, -0.25, 0, 0.25, 0.4, 0.5, 0.6, 1$ is shown through Figs. 3 – 10. Fig. 11 illustrates the variation of pressure gradient dp/dx for different value β . The pressure distribution over the entire range of x for different values of β is shown in Fig. 12. It is observed that velocity u decreases by increasing the non-Newtonian parameter over each of the cross-section $x = -0.5, -0.25, 0.25, 0.4, 0.5, 0.6$. However at cross-section $x = 0$ and $x = 1$ the situation is somewhat different. Here, the velocity u decreases near the center line while it increases over remainder of the cross-section by increasing β . Fig. 11 indicates that the magnitude of the pressure gradient at the nip point decreases by increasing β while it shows opposite behavior otherwise. The plot of pressure verses x shown through Fig. 12 reveals an increase in pressure by increasing β . The numerical values of sheet thickness exiting sheet thickness (H/H_0), power input (P_w) and roll separating force (F) are tabulated in Table 1 for different values of β . The numerical values of unknown eigen value of the problem λ are also given in Table. 1. It is observed that the leave-off distance, exiting sheet thickness, power input, and roll separating force increases by increasing β .

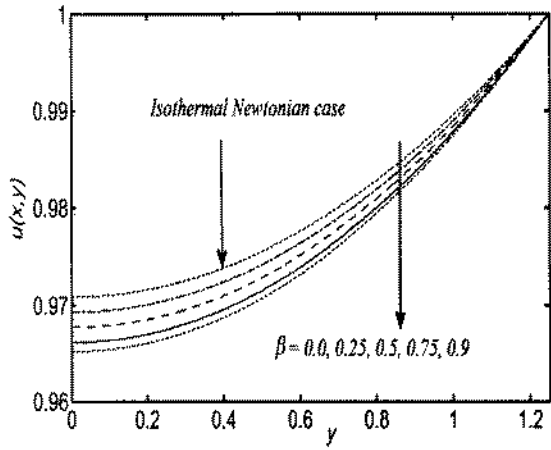


Fig. 3. Effect of β on velocity at $x = -0.5$.

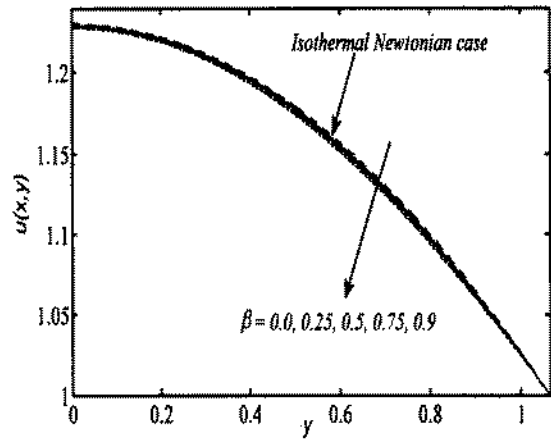


Fig. 4. Effect of β on velocity at $x = -0.25$.

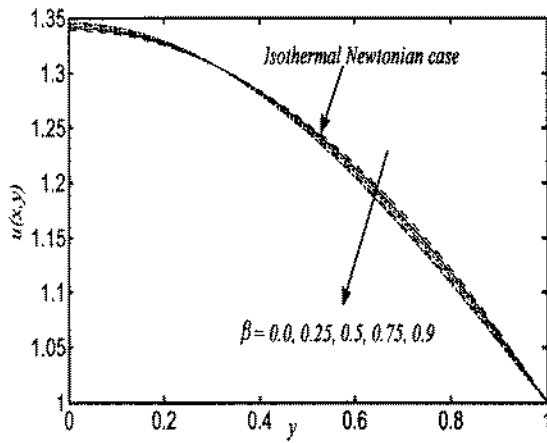


Fig. 5. Effect of β on velocity at $x = 0$.

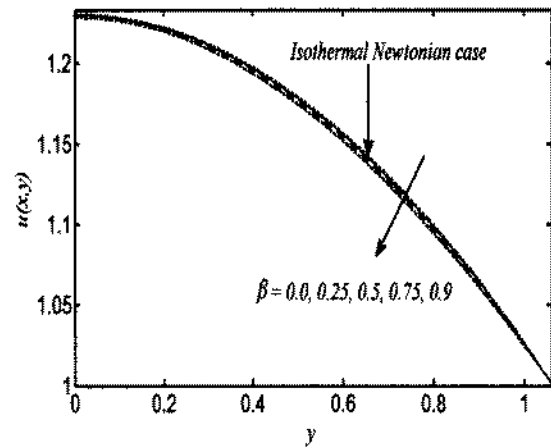


Fig. 6. Effect of β on velocity at $x = 0.25$.

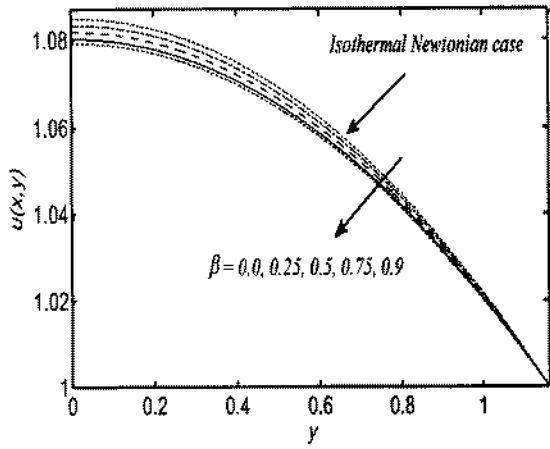


Fig. 7. Effect of β on velocity at $x = 0.4$.

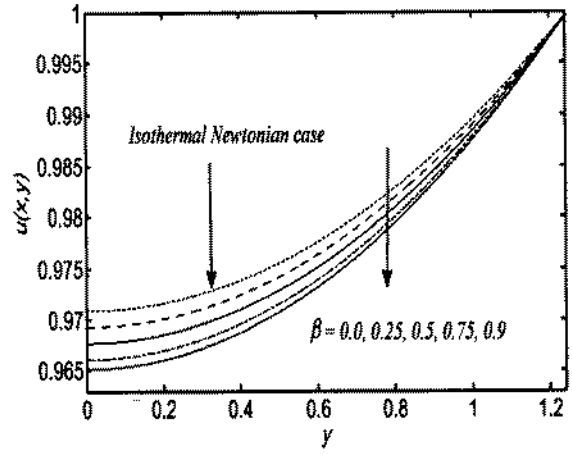


Fig. 8. Effect of β on velocity at $x = 0.5$.

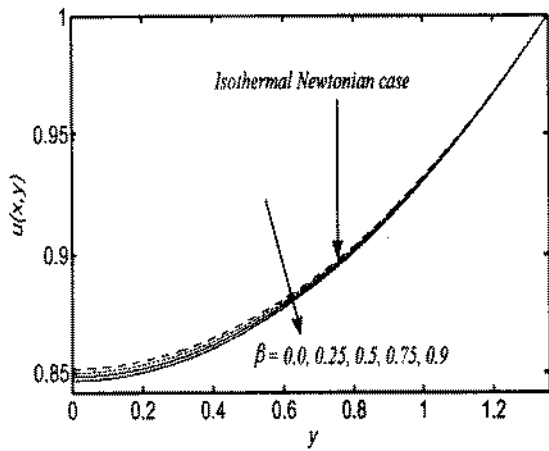


Fig. 9. Effect of β on velocity at $x = 0.6$.

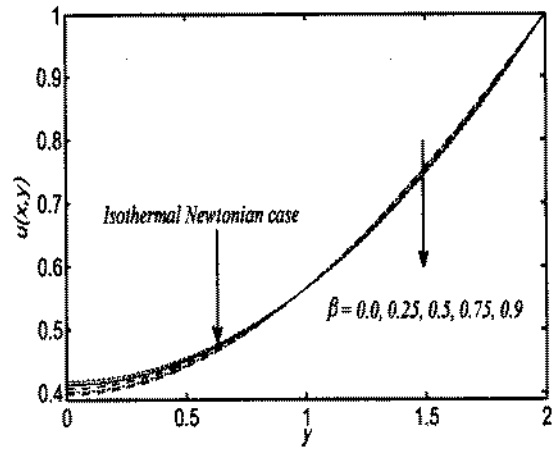


Fig. 10. Effect of β on velocity at $x = 1$.

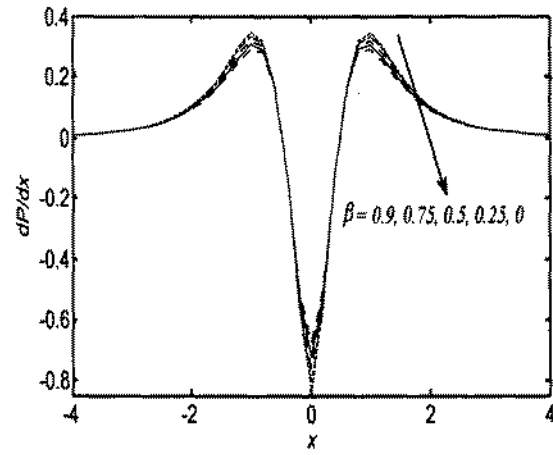


Fig. 11. Effect of β on pressure gradient.

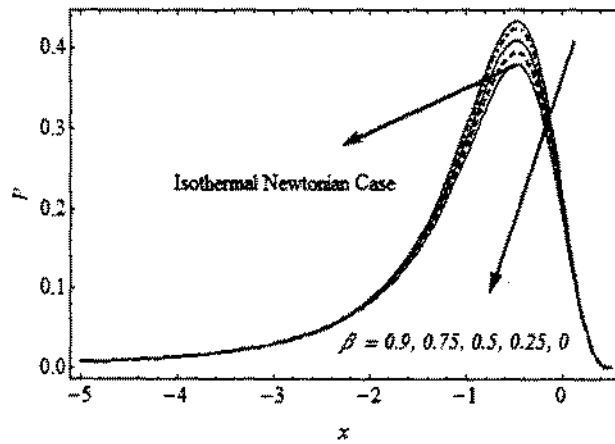


Fig. 12. Effect of β on pressure distribution.

Table 1. The effect of material parameter β on leave-off distance, final sheet thickness, power input and roll separating force

β	λ	Sheet thickness H/H_0	Power input ρ	Roll separating force ζ
0.01	0.4784	1.2289	0.0062	0.5527
0.03	0.4851	1.2353	0.0114	0.5542
0.05	0.4917	1.2418	0.0174	0.5557
0.07	0.4984	1.2484	0.0216	0.5572
0.09	0.5051	1.2551	0.0243	0.5587
0.1	0.5084	1.2585	0.0253	0.5594
0.3	0.5751	1.3308	0.0747	0.5744
0.5	0.6419	1.4120	0.1267	0.5901
0.7	0.7086	1.5021	0.1761	0.6068
0.9	0.7753	1.6011	0.2210	0.6248

$$\frac{\partial u}{\partial x} + \frac{\partial v}{\partial y} = 0, \quad (3.1)$$

$$\rho u \frac{\partial u}{\partial x} + \rho v \frac{\partial u}{\partial y} = -\frac{\partial p}{\partial x} + \frac{\partial \tau_{yx}}{\partial y}, \quad (3.2)$$

$$\rho u \frac{\partial v}{\partial x} + \rho v \frac{\partial v}{\partial y} = -\frac{\partial p}{\partial y} + \frac{\partial \tau_{xy}}{\partial x}. \quad (3.3)$$

For a simplified PTT fluids, τ_{yx} satisfies the following equation

$$\tau_{yx} + \frac{2\epsilon\lambda_f^2}{\eta}\tau_{yx}^2 \frac{\partial u}{\partial y} = \eta \frac{\partial u}{\partial y}, \quad (3.4)$$

where ϵ is the elongational parameter of the SPTT model, λ_f represents relaxation time and η represents polymer viscosity coefficient of the material. The polymer viscosity coefficient in term of zero-shear rate viscosity, η_0 is defined as $\eta = \eta_0 \left(1 + 2\epsilon\lambda_f^2 (\partial u/\partial y)^2\right)$. In the nip region and either side of it, the roll surfaces are nearly parallel when $H_0 \ll R$, thus allowing the lubrication approximation to be valid. Thus in the flow domain $v \ll u$ and $\frac{\partial u}{\partial x} \ll \frac{\partial u}{\partial y}$. The boundary conditions associated with Eqs. (3.1) – (3.3) are

$$y = 0 : \tau_{yx} = 0, \quad (3.5)$$

$$y = h(x) : u = U, \quad (3.6)$$

where the first condition represents the symmetry of the flow about the central plane while the second one is well-known no-slip condition to be satisfied by the fluid at roll surface. Let us scale the variables x, y and u as follows

$$x \sim L_c, y \sim H_0, u \sim \cdot \quad (3.7)$$

Utilizing the above relations in continuity equation, we get

$$\frac{v}{u} \sim \frac{H_0}{L_c} \ll 1, \quad (3.8)$$

The above relation indicates that order of magnitude of transversal velocity is smaller than longitudinal velocity. From expression (2.27) $L_c = \sqrt{2RH_0}$. The value of characteristic pressure can be obtained by performing an order of magnitude analysis on the basis of length and velocity scales defined above. This yields

$$p_c \sim \sqrt{\frac{2R}{H_0}} \frac{\mu_0}{H_0}. \quad (3.9)$$

3.2 Dimensionless equations

The above discussion allows us to define the following dimensionless variables

$$x^* = \frac{x}{\sqrt{2RH_0}}, \quad y^* = \frac{y}{H_0}, \quad p^* = \sqrt{\frac{H_0}{2R}} \frac{H_0 p}{\mu_0}, \quad u^* = \frac{u}{U}, \quad v^* = \sqrt{\frac{2R}{H_0}} \frac{v}{U}, \quad Q^* = \frac{Q}{2UH_0}. \quad (3.10)$$

In the above relationship Q represents the dimensionless volumetric flow rate which is constant. Using the above transformation Eqs. (3.1) – (3.3), after dropping the asteriks can be written as

$$\frac{\partial u}{\partial x} + \frac{\partial v}{\partial y} = 0, \quad (3.11)$$

$$Re \beta \left(u \frac{\partial u}{\partial x} + v \frac{\partial u}{\partial y} \right) = -\frac{\partial p}{\partial x} + \frac{\partial \tau_{xy}}{\partial y}, \quad (3.12)$$

$$Re \beta^2 \left(u \frac{\partial v}{\partial x} + v \frac{\partial v}{\partial y} \right) = -\frac{\partial p}{\partial y} + \beta \frac{\partial \tau_{xy}}{\partial x}. \quad (3.13)$$

In the above equation $\beta = (H_0/2R)^{1/2} \ll 1$ is a geometrical parameter, $Re = \rho U H_0 / \eta_0$ is the Reynolds number which for the typical calendering process is of order of 10^{-4} or 10^{-5} . This indicates that inertia plays a minor role this process. Neglecting the terms involving β and Re , Eqs. (3.12) and (3.13) reduce to:

$$\frac{dp}{dx} = \frac{\partial \tau_{xy}}{\partial y}, \quad (3.14)$$

and

$$\frac{\partial p}{\partial y} \approx 0. \quad (3.15)$$

The constitutive relation (3.4) in dimensionless form read:

$$\tau_{yx} + 2\epsilon We^2 \tau_{yx} \frac{\partial u}{\partial y} = \frac{\partial u}{\partial y}, \quad (3.16)$$

Here We is the Weissenberg number which is defined as $We = \lambda_f U / H_0$. It represents the ratio between elastic and viscous stresses. The dimensionless boundary condition are:

$$\tau_{yx} = 0 \quad \text{at} \quad y = 0, \quad (3.17)$$

$$u = 1 \quad \text{at} \quad y = 1 + x^2. \quad (3.18)$$

The boundary condition (3.17) and (3.18) are not sufficient to determine the pressure distribution. The additional conditions in the case of finite sheet examined here are as follows:

$$\frac{dp}{dx} = p = 0 \quad \text{at} \quad x = \lambda, \quad (3.19)$$

$$p = 0 \quad \text{at} \quad x = -x_f. \quad (3.20)$$

Eq. (3.15) shows that p is independent of y . Integration of Eq. (3.14) and after application of the boundary condition (3.17) and substitution of the result in Eq. (3.16) one gets

$$\left(\frac{dp}{dx}\right) y + \frac{\partial u}{\partial y} \left[2\epsilon We^2 \left(\frac{dp}{dx}\right)^2 y^2 - 1 \right] = 0. \quad (3.21)$$

The above equation along with the definition of the flow rate

$$Q = 1 + \lambda^2 = \int_0^{1+x^2} u dy \quad (3.22)$$

gives the complete description of the problem. In Eq. (3.22) λ is the unknown eigen value of the mathematical problem. It is related to exiting sheet thickness by the expression $\lambda^2 = H/H_0 - 1$. From the above equation it is desired to solve the flow problem in the regions, one where dp/dx is positive ($-x_f \leq x \leq -\lambda$) and the other where dp/dx is negative ($-\lambda \leq x \leq \lambda$). The next section is devoted to this task where the dimensionless velocity and pressure profiles are obtained for each region.

3.3 Perturbation solution

In this section, we determine the dimensionless velocity, pressure profiles and leave-off distance of the sheet for small values of the Weissenberg number using regular perturbation technique. To this end we propose the following expansions:

$$u = u_0 + We^2 u_1 + \dots, \quad (3.23)$$

$$p = p_0 + We^2 p_1 + \dots, \quad (3.24)$$

$$Q = Q_0 + We^2 Q_1 + \dots, \quad (3.25)$$

$$\lambda = \lambda_0 + We^2 \lambda_1 + \dots, \quad (3.26)$$

where the leading order solution u_0 , p_0 , Q_0 , and λ_0 represent the Newtonian case, whilst the corrections u_1 , p_1 , Q_1 , and λ_1 are the contribution of the viscoelastic effects. Substituting the above expansions into Eq. (3.21) and Eq. (3.22) and collecting the like power of We^2 , we obtain the following systems:

3.3.1 System of zeroth-order

$$\frac{dp_0}{dx} y = \frac{\partial u_0}{\partial y}, \quad -x_f \leq x \leq \lambda_0, \quad (3.27)$$

$$Q_0 = 1 + \lambda_0^2 = \int_0^{1+x^2} u_0 dy, \quad (3.28)$$

boundary conditions will be

$$\left\{ \begin{array}{ll} \tau_{yx,0} = 0 & \text{at } y = 0 \\ u_0 = 1 & \text{at } y = 1 + x^2 \\ \frac{dp_0}{dx} = p_0 = 0 & \text{at } x = \lambda_0 \\ p_0 = 0 & \text{at } x = -x_f \end{array} \right. \quad (3.29)$$

3.3.2 System of first-order

$$\left(\frac{dp_1}{dx} \right) y - \frac{\partial u_1}{\partial y} + 2\epsilon \left(\frac{dp_0}{dx} \right)^2 \frac{\partial u_0}{\partial y} y^2 = 0, \quad -x_f \leq x \leq \lambda_1, \quad (3.30)$$

$$Q_0 = 2\lambda_0\lambda_1 = \int_0^{1+x^2} u_1 dy \quad (3.31)$$

boundary conditions will be

$$\begin{cases} \tau_{yx,1} = 0 & \text{at } y = 0 \\ u_1 = 0 & \text{at } y = 1 + x^2 \\ p_1 = 0 & \text{at } x = -x_f \\ \frac{dp_1}{dx} = p_1 = 0 & \text{at } x = \lambda_1 \end{cases} \quad (3.32)$$

3.3.3 Zeroth-order solution

The solution for Eq. (3.27) and Eq. (3.28) is given by:

$$u_0 = 1 + \frac{1}{2} \left(\frac{dp_0}{dx} \right) \left[y^2 - (1 + x^2)^2 \right], \quad (3.33)$$

with

$$\frac{dp_0}{dx} = -3 \frac{(\lambda_0^2 - x^2)}{(1 + x^2)^3}, \quad \text{for } x_f \leq x < \lambda_0. \quad (3.34)$$

Integration of (3.34) and using $p_0(\lambda_0) = 0$ gives

$$p_0(x) = \frac{3}{8} \left[\frac{x^2(1 - 3\lambda_0^2) - 1 - 5\lambda_0^2}{(1 + x^2)^2} x + (1 - 3\lambda_0^2) (\arctan[x] - \arctan[\lambda_0]) + \frac{1 + 3\lambda_0^2}{1 + \lambda_0^2} \lambda_0 \right], \quad (3.35)$$

From above equation, the value of λ_0 which is related to final sheet thickness is obtained by using the condition $p_0(-x_f) = 0$. This gives

$$0 = -\frac{2\lambda_0}{(1+\lambda_0^2)} \left(\frac{\lambda_0}{1+\lambda_0^2} + \arctan(\lambda_0) \right) (1 - 3\lambda_0^2) - (1 - 3\lambda_0^2) \left[\frac{(H_f/H_0 - 1)^{1/2}}{H_f/H_0} + \arctan \left((H_f/H_0 - 1)^{1/2} \right) \right] + 2 \frac{(1+\lambda_0^2)(H_f/H_0 - 1)^{1/2}}{(H_f/H_0)^2}. \quad (3.36)$$

Taking $-x_f$ sufficient large, which corresponds to the case of infinite reservoir of fluid upstream from the nip region, it is found that $\lambda_0 = 0.4751$. This value is exactly the same as found in section 2.2.3 of chapter 2. Since the introduction of the transformation $Y = y/(1 + x^2)$,

facilities the examination of velocity distribution in easy manner, therefore the zeroth-order velocity profile can be expressed as

$$u_0 = 1 + \frac{3}{2}(Y^2 - 1), \quad \text{for all } dp_0/dx. \quad (3.37)$$

3.3.4 First-order solution

In this sub section we intend to find the correction to the leading order solution of the dimensionless velocity, pressure profile and the final sheet thickness due to non-Newtonian effects. To this end we integrate Eq. (3.30) substituting the expression of dp_0/dx and get

$$u_1 = \frac{1}{2} \frac{dp_1}{dx} y^2 + \frac{54}{4} \epsilon \frac{(x^2 - \lambda_0^2)^3}{(1 + x^2)^9} y^4 + C_1(x), \quad (3.38)$$

where $C_1(x)$ is an integration constant. The above expression in term of the variable Y after applying the boundary conditions (3.32) takes the form

$$u_1(x, Y) = \frac{1}{2} \frac{dp_1}{dx} (1 + x^2)^2 [Y^2 - 1] + \frac{54}{4} \epsilon \frac{(x^2 - \lambda_0^2)^3}{(1 + x^2)^5} [Y^4 - 1]. \quad (3.39)$$

Insertion of (3.39) in. (3.31) gives

$$Q_1 = -\frac{1}{3} \frac{dp_1}{dx} (1 + x^2)^3 - \frac{54}{5} \epsilon \frac{(x^2 - \lambda_0^2)^3}{(1 + x^2)^4}. \quad (3.40)$$

The left hand side of Eq. (3.40) is unknown. To find the value of Q_1 , we apply the boundary condition $dp_1/dx = 0$ at $x = \lambda_1$. This gives

$$Q_1 = -\frac{54}{5} \epsilon \frac{(\lambda_1^2 - \lambda_0^2)^3}{(1 + \lambda_1^2)^4}. \quad (3.41)$$

Using the above value of Q_1 in (3.40) and after doing some algebra we end up with th following expression dp_1/dx :

$$\frac{dp_1}{dx} = \frac{162}{5} \epsilon \left[\frac{(\lambda_1^2 - \lambda_0^2)^3}{(1 + x^2)^3 (1 + \lambda_1^2)^4} - \frac{(x^2 - \lambda_0^2)^3}{(1 + x^2)^7} \right], \quad (3.42)$$

valid in the region $-x_f \leq x < \lambda_1$. Integration of above expression yield the pressure distribution

$$p_1(x) = \frac{162}{5} \epsilon \int_{-x_f}^x \left[\frac{(\lambda_1^2 - \lambda_0^2)^3}{(1+x^2)^3 (1+\lambda_1^2)^4} - \frac{(x^2 - \lambda_0^2)^3}{(1+x^2)^7} \right] dx. \quad (3.43)$$

The dimensionless leave-off distance λ_1 may be found from Eq. (3.43) by using the condition $p_1 = 0$ at $x = -x_f$ i.e

$$0 = \int_{-x_f}^{\lambda_1} \left[\frac{(\lambda_1^2 - \lambda_0^2)^3}{(1+x^2)^3 (1+\lambda_1^2)^4} - \frac{(x^2 - \lambda_0^2)^3}{(1+x^2)^7} \right] dx. \quad (3.44)$$

The explicit expression of pressure after integrating Eq. (3.43) and using boundary condition (3.32) turn out to be

$$\begin{aligned} p_1(x) = & \frac{162}{5} \epsilon \left[\frac{x(\lambda_0^6 + 3\lambda_0^4 + 3\lambda_0^2 + 1)}{12(1+x^2)^6} + \frac{x(11\lambda_0^6 - 3\lambda_0^4 - 39\lambda_0^2 - 25)}{120(1+x^2)^5} + \frac{3x(11\lambda_0^6 - 3\lambda_0^4 + \lambda_0^2 + 15)}{320(1+x^2)^4} \right. \\ & + \frac{x(231\lambda_0^6 - 63\lambda_0^4 + 21\lambda_0^2 - 5)}{1920(1+x^2)^3} + \frac{x(231\lambda_0^6 - 63\lambda_0^4 + 21\lambda_0^2 - 5)}{1536(1+x^2)^2} + \frac{x(231\lambda_0^6 - 63\lambda_0^4 + 21\lambda_0^2 - 5)}{1024(1+x^2)} \\ & + \frac{x(\lambda_1^2 - \lambda_0^2)^3}{4(1+x^2)^2(1+\lambda_1^2)^4} + \frac{3x(\lambda_1^2 - \lambda_0^2)^3}{8(1+x^2)(1+\lambda_1^2)^4} + \frac{(231\lambda_0^6 - 63\lambda_0^4 + 21\lambda_0^2 - 5) \arctan(x)}{1024} \\ & \left. + \frac{3(\lambda_1^2 - \lambda_0^2)^3 \arctan(x)}{8(1+\lambda_1^2)^4} + \sqrt{\frac{H_f}{H_0} - 1} \left(\frac{(\lambda_0^6 + 3\lambda_0^4 + 3\lambda_0^2 + 1)}{12\left(\frac{H_f}{H_0}\right)^6} + \frac{(11\lambda_0^6 - 3\lambda_0^4 - 39\lambda_0^2 - 25)}{120\left(\frac{H_f}{H_0}\right)^5} \right. \right. \\ & + \frac{3(11\lambda_0^6 - 3\lambda_0^4 + \lambda_0^2 + 15)}{320\left(\frac{H_f}{H_0}\right)^4} + \frac{(231\lambda_0^6 - 63\lambda_0^4 + 21\lambda_0^2 - 5)}{1920\left(\frac{H_f}{H_0}\right)^3} + \frac{(231\lambda_0^6 - 63\lambda_0^4 + 21\lambda_0^2 - 5)}{1536\left(\frac{H_f}{H_0}\right)^2} \\ & + \frac{(231\lambda_0^6 - 63\lambda_0^4 + 21\lambda_0^2 - 5)}{1024\left(\frac{H_f}{H_0}\right)} + \frac{(\lambda_1^2 - \lambda_0^2)^3}{4\left(\frac{H_f}{H_0}\right)^2(1+\lambda_1^2)^4} + \left. \frac{3(\lambda_1^2 - \lambda_0^2)^3}{8\left(\frac{H_f}{H_0}\right)(1+\lambda_1^2)^4} \right) \\ & \left. \frac{(231\lambda_0^6 - 63\lambda_0^4 + 21\lambda_0^2 - 5) \arctan\left(\sqrt{\frac{H_f}{H_0} - 1}\right)}{1024} + \frac{3(\lambda_1^2 - \lambda_0^2)^3 \arctan\left(\sqrt{\frac{H_f}{H_0} - 1}\right)}{8(1+\lambda_1^2)^4} \right] \quad (3.45) \end{aligned}$$

Similarly, performing integration in Eq. (3.44) result in the following determining equation for

λ_1

$$\begin{aligned}
0 = & \sqrt{\frac{H_f}{H_0}} - 1 \left(\frac{(\lambda_0^6 + 3\lambda_0^4 + 3\lambda_0^2 + 1)}{12 \left(\frac{H_f}{H_0}\right)^6} + \frac{(11\lambda_0^6 - 3\lambda_0^4 - 39\lambda_0^2 - 25)}{120 \left(\frac{H_f}{H_0}\right)^5} + \frac{3(11\lambda_0^6 - 3\lambda_0^4 + \lambda_0^2 + 15)}{320 \left(\frac{H_f}{H_0}\right)^4} \right. \\
& + \frac{(231\lambda_0^6 - 63\lambda_0^4 + 21\lambda_0^2 - 5)}{1920 \left(\frac{H_f}{H_0}\right)^3} + \frac{(231\lambda_0^6 - 63\lambda_0^4 + 21\lambda_0^2 - 5)}{1536 \left(\frac{H_f}{H_0}\right)^2} + \frac{(231\lambda_0^6 - 63\lambda_0^4 + 21\lambda_0^2 - 5)}{1024 \left(\frac{H_f}{H_0}\right)} \\
& + \frac{(\lambda_1^2 - \lambda_0^2)^3}{4 \left(\frac{H_f}{H_0}\right)^2 (1 + \lambda_1^2)^4} + \frac{3(\lambda_1^2 - \lambda_0^2)^3}{8 \left(\frac{H_f}{H_0}\right) (1 + \lambda_1^2)^4} + \frac{(231\lambda_0^6 - 63\lambda_0^4 + 21\lambda_0^2 - 5) \arctan\left(\sqrt{\frac{H_f}{H_0}} - 1\right)}{1024} + \\
& \left. \frac{3(\lambda_1^2 - \lambda_0^2)^3 \arctan\left(\sqrt{\frac{H_f}{H_0}} - 1\right)}{8(1 + \lambda_1^2)^4} \right) + \left(\frac{\lambda_1(\lambda_0^6 + 3\lambda_0^4 + 3\lambda_0^2 + 1)}{12(1 + \lambda_1^2)^6} + \frac{\lambda_1(11\lambda_0^6 - 3\lambda_0^4 - 39\lambda_0^2 - 25)}{120(1 + \lambda_1^2)^5} \right. \\
& + \frac{3\lambda_1(11\lambda_0^6 - 3\lambda_0^4 + \lambda_0^2 + 15)}{320(1 + \lambda_1^2)^4} + \frac{\lambda_1(231\lambda_0^6 - 63\lambda_0^4 + 21\lambda_0^2 - 5)}{1920(1 + \lambda_1^2)^3} + \frac{\lambda_1(231\lambda_0^6 - 63\lambda_0^4 + 21\lambda_0^2 - 5)}{1536(1 + \lambda_1^2)^2} \\
& + \frac{\lambda_1(231\lambda_0^6 - 63\lambda_0^4 + 21\lambda_0^2 - 5)}{1024(1 + \lambda_1^2)} + \frac{\lambda_1(\lambda_1^2 - \lambda_0^2)^3}{4(1 + \lambda_1^2)^6} + \frac{3\lambda_1(\lambda_1^2 - \lambda_0^2)^3}{8(1 + \lambda_1^2)^5} \\
& \left. + \frac{(231\lambda_0^6 - 63\lambda_0^4 + 21\lambda_0^2 - 5) \arctan(\lambda_1)}{1024} + \frac{3(\lambda_1^2 - \lambda_0^2)^3 \arctan(\lambda_1)}{8(1 + \lambda_1^2)^4} \right). \quad (3.46)
\end{aligned}$$

Now for given value of H_f/H_0 , the corresponding value of λ_0 can be found through Eq. (3.36) and then using this value we may consecutively obtain λ_1 and p_1 from Eqs. (3.46) and (3.45), respectively.

3.4 Numerical solution

The solution in previous section was valid for small values of Weissenberg number We . To obtain solution for large values of We , we outline in this section a numerical algorithm is based on Runge-Kutta method. Integration of Eq. (3.21) and application of boundary condition

(3.17) and (3.18) yields :

$$u = 1 + \frac{1}{2} \frac{dp}{dx} \left(\frac{y^2}{1 - 2\epsilon W e^2 \left(\frac{dp}{dx}\right)^2 y^2} - \frac{(1+x^2)^2}{1 - 2\epsilon W e^2 \left(\frac{dp}{dx}\right)^2 (1+x^2)^2} \right). \quad (3.47)$$

Using Eq. (3.47) in Eq. (3.22) gives the volumetric flow rate

$$Q = 1 + x^2 - \frac{1}{5} \frac{dp}{dx} (1+x^2)^3 \left(\frac{2}{3 \left(1 - 2\epsilon W e^2 \left(\frac{dp}{dx}\right)^2\right)} + \frac{1}{1 - 2\epsilon W e^2 \left(\frac{dp}{dx}\right)^2 (1+x^2)^2} \right). \quad (3.48)$$

Application of boundary condition $dp/dx = 0$ at $x = \lambda$ gives:

$$Q = 1 + \lambda^2. \quad (3.49)$$

Substituting value of Q from Eq. (3.49) in (3.48), we get the following implicit expression for dp/dx .

$$\frac{dp}{dx} = -2 \frac{(\lambda^2 - x^2)}{(1+x^2)^3} \left[\frac{\left(1 - 2\epsilon W e^2 \left(\frac{dp}{dx}\right)^2 (1+x^2)^2\right)^2}{\frac{4}{15} + \frac{2}{5} \left(1 - 2\epsilon W e^2 \left(\frac{dp}{dx}\right)^2 (1+x^2)^2\right)} \right], \quad (3.50)$$

From Eq. (3.50), the pressure distribution is represented by

$$p(x) = 2 \int_{\lambda}^x \frac{(x^2 - \lambda^2)}{(1+x^2)^3} \left[\frac{\left(1 - 2\epsilon W i^2 \left(\frac{dp}{dx}\right)^2 (1+x^2)^2\right)^2}{\frac{4}{15} + \frac{2}{5} \left(1 - 2\epsilon W i^2 \left(\frac{dp}{dx}\right)^2 (1+x^2)^2\right)} \right] dx. \quad (3.51)$$

Now, from Eq. (3.51) pressure distribution can be obtained as a function of x by assuming λ and We to be known. Any root finding algorithm can be used to obtain the values of pressure gradient at each longitudinal location x . Now to find the value of local pressure, we integrate dp/dx using Runge-Kutta method starting from $x = \lambda$ and applying the boundary condition $p = 0$ at $x = \lambda$. The integration carried out until the pressure becomes negative. The corresponding value of x gives the location of $-x_f$, where entering sheet bites the rolls and from which the thickness of entering sheet can be found through the relation $x_f = (H_f/H_o - 1)^{1/2}$.

A step size of Δx is 0.001.is chosen in all the simulation's.

3.5 Roll separating force

The force separating the two rolls is given by the expression

$$\frac{F}{W} (We) = \frac{\mu_o UR}{H_o} \mathfrak{S} (We), \quad (3.52)$$

where W is the width of rolls and $\mathfrak{S} (We)$ is the dimensionless force function given by

$$\zeta (We) = 6 \int_{-x_f}^{\lambda} \left[\int_x^{\lambda} \Gamma (We) dx \right] dx. \quad (3.53)$$

in which

$$\Gamma (We) = \frac{2 (\lambda^2 - x^2)}{3 (1 + x^2)^3} \left[\frac{\left(1 - 2\epsilon W i^2 \left(\frac{dp}{dx} \right)^2 (1 + x^2)^2 \right)^2}{\frac{4}{15} + \frac{2}{5} \left(1 - 2\epsilon W i^2 \left(\frac{dp}{dx} \right)^2 (1 + x^2)^2 \right)} \right]. \quad (3.54)$$

3.6 Power input

The power transmitted to the fluid by the rolls can be found by integrating the roll velocity and shear stress along the surface of roll

$$\hat{w} (We) = W U^2 \mu_o \sqrt{\frac{R}{H}} \wp (We), \quad (3.55)$$

where $\wp (We)$ is the dimensionless power function, which is given by

$$\wp (We) = -6\sqrt{2} \int_{-x_f}^{\lambda} \Gamma (We) (1 + x^2) dx. \quad (3.56)$$

3.7 Graphical results and discussion

In this section, graphical results are displayed in order to analyze the effect of Weissenberg number on velocity distribution, pressure gradient, longitudinal pressure profile, roll separation force and power input function. Figs 1 and 2 are plotted to see the influence of Weissenberg number on longitudinal distribution of pressure gradient for $\lambda = 0.2923$ and $\lambda = 0.440$, respectively. It is observed that as a result of imposed boundary condition the pressure gradient is zero at $x = \lambda$, the location where sheet exit from the rolls. Moving left to this point result in negative values of pressure gradient with a minimum occurring at $x = 0$. Beyond this point, the pressure gradient begin to rise reaching to zero at $x = -\lambda$ and from here it continues to increase to a maximum at $x = -x_f$ in some cases while in other the maximum is achieved before the entry point. The maximum deviation in pressure gradient with respect to Weissenberg number is seen at the nip region i.e $x = 0$. However, near $x = \pm\lambda$ the effects of Weissenberg number are not pronounced. It is further observed that an increase in Weissenberg number result in decrease of pressure gradient in the neighborhood of $x = 0$ and $x = -x_f$. The profiles of dimensionless pressure distribution in the domain $-x_f \leq x \leq \lambda$ for various values of Weissenberg number are shown in Figs. 3 and 4 for $\lambda = 0.2923$ and $\lambda = 0.440$, respectively. It is observed that pressure monotonically increases from zero at $x = \lambda$ to a maximum at $x = -\lambda$ and then decreases to zero at the entry point $x = -x_f$. Moreover, the maximum deviation in pressure with respect to Weissenberg number occurs at $x = -\lambda$. It is found from the present calculations that for the case of $\lambda = 0.440$ and $We = 0.9$ (Fig. 4) the value of pressure at $x = -\lambda$ is 36% less than its corresponding value for $\lambda = 0.440$ and $We = 0$. As an implication of this decrease in pressure by increasing Weissenberg number, the point $-x_f$ where sheet first bites the rolls is further shifted to left resulting in extension of length of contact between the rolls and the fluid. The dimensionless velocity u at two axial stations $x = -0.6$ ($dp/dx > 0$) and $x = 0.1$ ($dp/dx < 0$) for different values of λ is shown through Figs. 5 and 6. It is observed that for the case when ($dp/dx > 0$) the dimensionless velocity u increases with the Weissenberg number. Moreover, the effects of Weissenberg number on u are more pronounced at the centerline. On the contrary, such effects diminish in the vicinity of the rolls. The variation of u with Weissenberg number at axial location $x = 0.1$ where $dp/dx < 0$ is shown in Fig. 6. It is evident from Fig. 6 that u decreases at center plane with Weissenberg number while it shows

opposite trend near the rolls. Fig. 7 presents a comparison of numerical values of λ obtained through numerical and analytical solutions as a function of entering sheet thickness H_f/H_0 for $We = 0.08$. This figure indicates an excellent correlation between the result obtained via both solutions. Fig. 8 shows the plot of λ obtained via numerical solution as a function of H_f/H_0 for different values of Weissenberg number. It is noted that $H_f/H_0 < 10$, viscoelastic effects tend to decrease the sheet thickness. However for $H_f/H_0 > 10$ an opposite trend is observed i.e viscoelastic effects produce an enhancement in the sheet thickness. The roll separating force and power transmitted to the fluid by the rolls as a function of We and for different values of λ are plotted in Figs 9 and 10 respectively. It is observed that for a fixed value of λ , an increase in Weissenberg number causes a decrease in the dimensionless roll separating force. Similar observations is made for the case of dimensionless power transmitted to the rolls. It is further noted that each of these variables is also a decreasing function of leave-off distance λ .

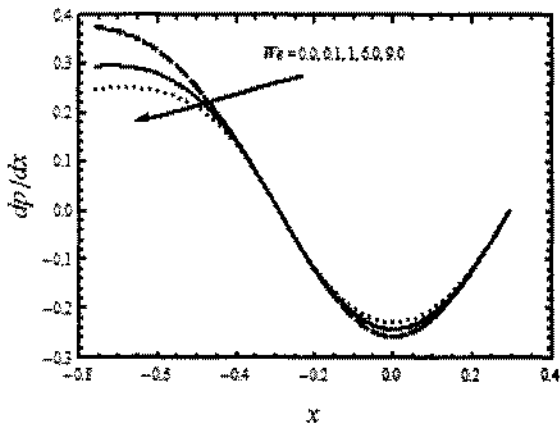


Fig. 1. The longitudinal distribution of dp/dx for different values of We with $\lambda = 0.2923$.

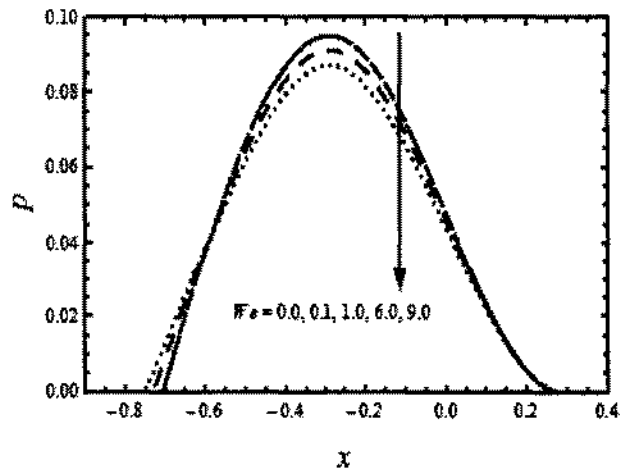


Fig. 3. The longitudinal distribution of pressure for different values of We with $\lambda=0.2923$.

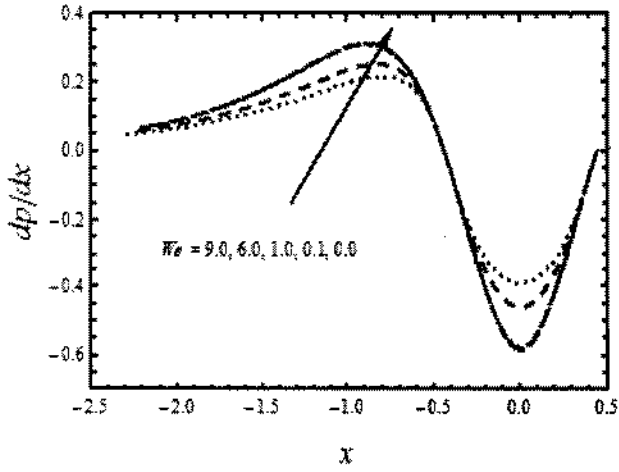


Fig. 2. The longitudinal distribution of dp/dx for various values of We with $\lambda = 0.440$.

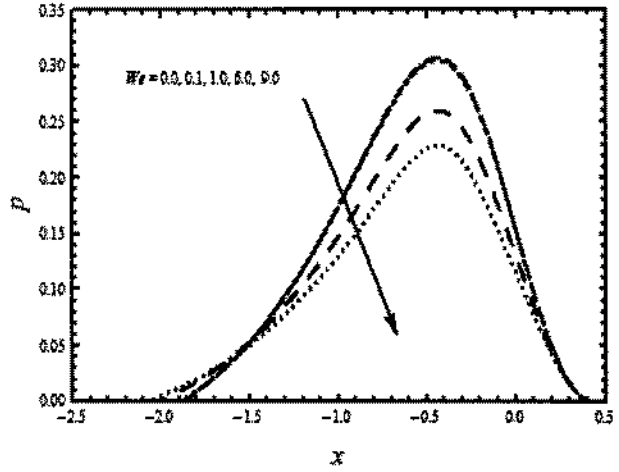


Fig. 4. The longitudinal distribution of pressure for different values of We with $\lambda = 0.440$.

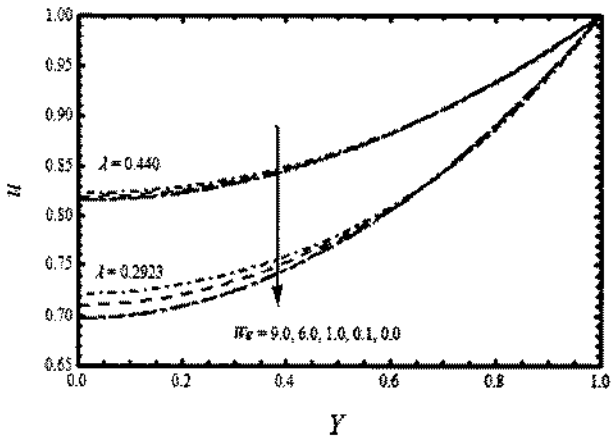


Fig. 5. Transverse distribution of velocity for different values of We for two different values of λ when $dp/dx > 0$ and $x = -0.6$.

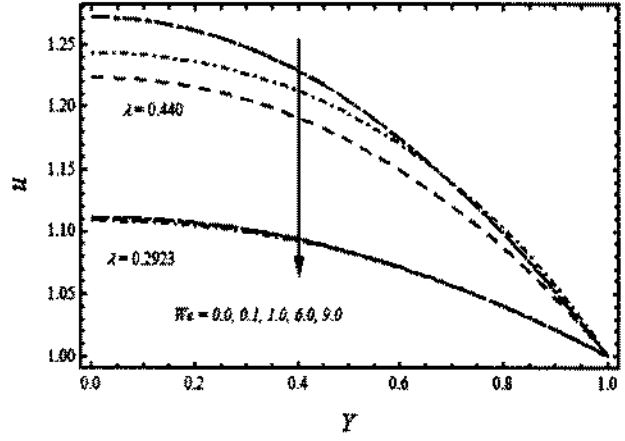


Fig. 6. Transverse distribution of velocity for different values of We for two different values of λ when $dp/dx < 0$ and $x = 0.1$.

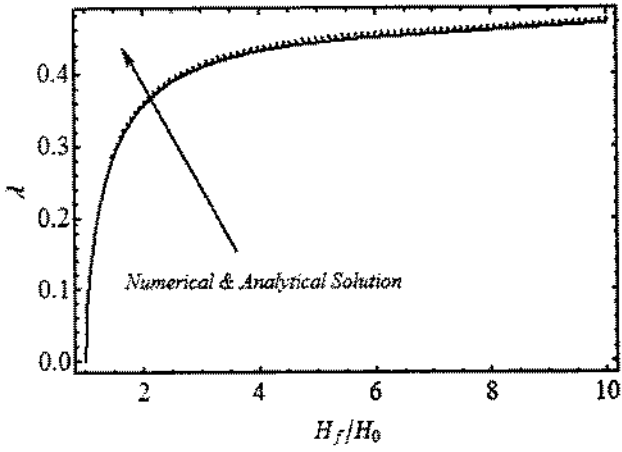


Fig. 7. Plot showing λ obtained through numerical solution and analytical solution as a function H_f/H_0 for $We = 0.08$.

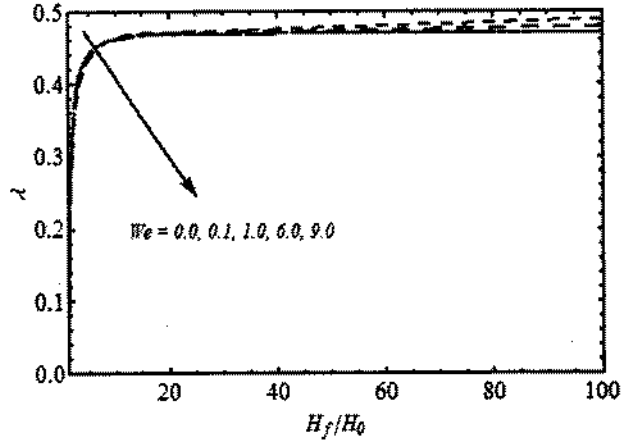


Fig. 8. Plot showing λ obtained through numerical solution as a function H_f/H_0 for various values of We .

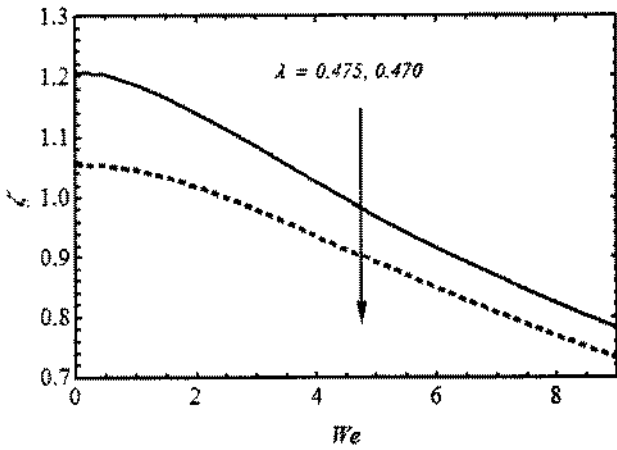


Fig. 9. Roll separating force as a function of Weissenberg number for two different values of λ .

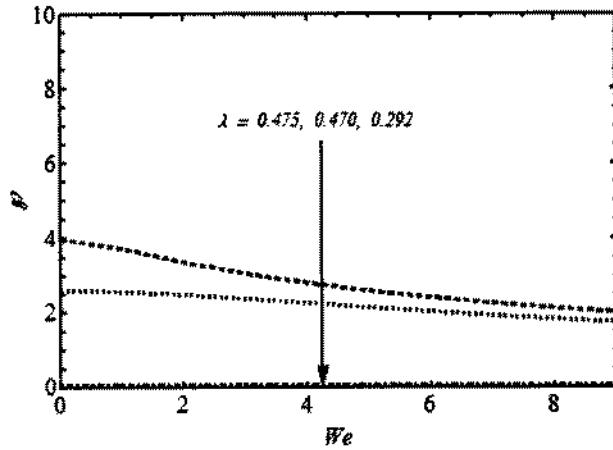


Fig. 10. Power transmitted to the fluid by the rolls as a function of Weissenberg number for three different values of λ .

Bibliography

- [1] R.E. Gaskell, The calendering of plastic materials, *Journal of Applied Mech.* (1950); 17 : 334 – 336.
- [2] J.M. McKelvey, *Poly. Pro.* (1962); Wiley, New York.
- [3] S. Middlemen, *Fundamental of polymer processing.* (1977); McGraw-Hill, New York.
- [4] S. Sofou, E. Mitsoulis, Calendering of pseudoplastic and viscoplastic sheets of finite thickness, *Journal of Plastic Film and Sheeting* (2004); 20 : 185 – 222.
- [5] E. Mitsoulis, Numerical simulation of calendering viscoplastic fluids, *Journal of Non-Newtonian Fluid Mechanics* (2008); 154 : 77 – 88.
- [6] F. Dobbels, J. Mewis, Nonisothermal nip flow in calendering operation, *AIChE Journal* (1977); 23 : 224 – 232.
- [7] C. Kiparissides, J. Vlachopoulos, A study of viscous dissipation in the calendering of power-law fluids, *Polym. Eng. Sci.* (1978); 18 : 210 – 214.
- [8] J.C. Arcos, F. Méndez, O. Bautista, Effect of temperature-dependent consistency index on the exiting sheet thickness in the calendering of power-law fluids, *International Journal of Heat and Mass Transfer* (2011); 54 : 3979 – 3986.
- [9] R. Zheng, R.I. Tanner, A numerical analysis of calendering, *Journal of Non-Newtonian Fluid Mechanics* (1988); 28 : 149 – 170.

- [10] J.C. Arcos, O. Bautista, F. Mendez and E.G. Bautista, Theoretically analysis of the Calendered exiting thickness of viscoelastic sheets. *Journal of Non-Newtonian Fluid Mechanics* (2012); 29 – 36.
- [11] A.M. Siddiqui, M. Zahid, M.A. Rana and T. Haroon, Calendering analysis of third order fluid. *Journal of Plastic Film and Sheeting* (2013); 0 : 1 – 24.
- [12] R.L. Fosdick and K.R. Rajagopal, Thermodynamics and stability of fluids of third grade. *Proc R Soc.* (1980); 22 : 351 – 377.